Earthline Journal of Chemical Sciences
E-ISSN: 2581-9003; CODEN: EJCSB4
Volume 13, Number 3, August 2026, Pages 231-244
https://doi.org/10.34198/ejcs.13326.18.231244

Inhibition of aluminum corrosion in hydrochloric acid medium by 2-(2-(4chlorobenzylidene)hydrazinyl)-3-nitroimidazo[1,2-a]pyridine: gravimetric and adsorption studies

Tanoh Stanley KOUAME

Laboratoire de Réaction et Constitution de la Matière, Université Félix Houphouët BOIGNY, 22 BP 582 Abidjan 22, Côte d'Ivoire

Ahissan Donatien EHOUMAN*

Laboratoire de Thermodynamique et Physico-Chimie du Milieu, Université NANGUI ABROGOUA, 02 BP 801 Abidjan 02, Côte d'Ivoire
e-mail: ehoumandona@gmail.com

Kossitse Venyo AKPATAKU

Laboratoire de Chimie Organique et Sciences Environnementales, Faculté de Science et Technologie, Université de Kara, BP 404, Kara, Togo

Paulin Marius NIAMIEN

Laboratoire de Réaction et Constitution de la Matière, Université Félix Houphouët BOIGNY, 22 BP 582 Abidjan 22, Côte d'Ivoire

Abstract

The purpose of this study is to evaluate the corrosion-inhibiting efficacy of the 2-(2-(4-chlorobenzylidene)hydrazinyl)-3-nitroimidazo[1,2-α] pyridine, or 4Cl-BNH-NIP, on aluminum corrosion in a 1 M hydrochloric acid medium using the gravimetric method. The corrosion inhibition efficiency increases with inhibitor concentration but decreases with increasing temperature. Adsorption isotherm models (Langmuir, El-Awady, Freundlich, Flory-Huggins, Frunkin, and Temkin) were used to describe the interactions between the molecule and metallic aluminum. The Dubinin-Radushkevich and Adejo-Ekwenchi isotherms were used to identify the adsorption modes. The thermodynamic parameters of adsorption and activation were also determined and analyzed in this study.

1. Introduction

Aluminum [1,2] is one of the most widely used metals in public infrastructure, industry (food, chemical, and petroleum), and the transportation sector due to its remarkable physical, mechanical, and physicochemical properties. However, despite these advantages, it remains vulnerable to corrosion, particularly in acidic and chlorinated environments [3,4]. Corrosion is a major problem with significant economic, environmental, and safety impacts, accounting for approximately 3.4% of global GDP in costs related to maintenance, equipment replacement, and production downtime [5,6]. In light of these challenges, the use of corrosion inhibitors has emerged as an effective strategy for protecting metals. Among these solutions, organic inhibitors, particularly those in the benzimidazole family, have garnered growing interest due to their effectiveness and environmental

Received: April 12, 2026; Revised & Accepted: May 28, 2026; Published online: June 5, 2026

Keywords and phrases: aluminum, 2-(2-(4-chlorobenzylidene)hydrazinyl)-3-nitroimidazo[1,2-α]pyridine, corrosion inhibition, gravimetric, adsorption.

*Corresponding author

Copyright © 2026 the Authors

friendliness [7]. Several recent studies have shown that these compounds exhibit good adsorption properties on metal surfaces, thereby reducing the corrosion rate [7,8]. The evaluation of inhibitory performance is generally carried out using gravimetric and electrochemical methods, which provide macroscopic information on the corrosion phenomenon [9]. The objective of this work is to study the inhibitory efficacy of a benzimidazole-type organic compound, namely 4Cl-BNH-NIP, against aluminum corrosion in a 1 M hydrochloric acid medium. This study aims to identify an effective and environmentally friendly corrosion inhibitor.

2. Materials and Methods

2.1. Aluminum Specimens

The aluminum specimens were cylindrical rods measuring 10 mm in length and 2 mm in diameter. They consist of commercial aluminum with a purity of 98 %. The molecule under study, 2-(2-(4-chlorobenzylidene)hydrazineyl)-3-nitroimidazo[1,2-α] pyridine, or 4Cl-BNH-NIP, is a molecule synthesized and obtained by the aldolization of 2-hydrazineyl-3-nitroimidazo[1,2-α]pyridine with 99.99% pure 4-chlorobenzaldehyde. Its molar mass is M = 315.72 g/mol, and its molecular formula is $C_{14}H_{10}ClN_5O_2$.

Figure 1 shows the molecular structure of 4Cl-BNH-NIP.

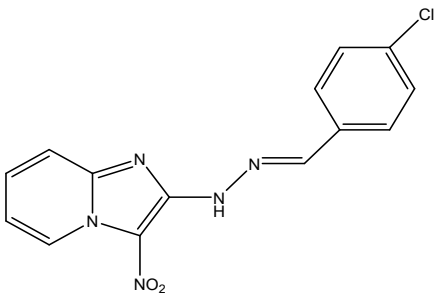

(*E*)-2-(2-(4-chlorobenzylidene)hydrazineyl)-3-nitroimidazo[1,2-*a*]pyridine

Figure 1. molecular structure of 4Cl-BNH-NIP.

2.2. Prepared Solutions

A hydrochloric acid solution was prepared by diluting a commercial 1 M hydrochloric acid solution with distilled water. The hydrochloric acid has the following properties: d = 1.19 g/mL and P = 37%. The prepared 4Cl-BNH-NIP solutions have concentrations of C = 0.001 mM, C = 0.005 mM, C = 0.01 mM, C = 0.05 mM, C = 0.1 mM, and C = 0.5 mM.

2.3. Mass Loss Method

The gravimetric method [10–12] is commonly used to study corrosion inhibition due to its simplicity and the reliability of the results obtained. It involves completely immersing a pre-weighed metal sample in a test solution contained in a beaker, at temperatures ranging from 298 K to 338 K. After a defined exposure time, the sample is removed, carefully rinsed with distilled water, and then reweighed using a precision balance. The average mass losses thus obtained allow for the determination of essential parameters such as corrosion rate, inhibitory efficiency, and coverage rate using appropriate equations.

$$W = \frac{\Delta m}{St} \tag{1}$$

$$EI(\%) = \frac{W_0 - W}{W_0} \times 100 \tag{2}$$

$$\theta = \frac{W_0 - W}{W_0} \quad (3)$$

where W_0 and W are the corrosion rates in the absence and presence of the inhibitor, respectively. Δm is the mass loss, S is the total surface area of the aluminium sample, and t is the immersion time.

3. Results and Discussion

3.1. Effects of Concentration and Temperature

Figures 2 and 3 show, respectively, the variation in the corrosion inhibition rate as a function of temperature and 4Cl-BNH-NIP concentration.

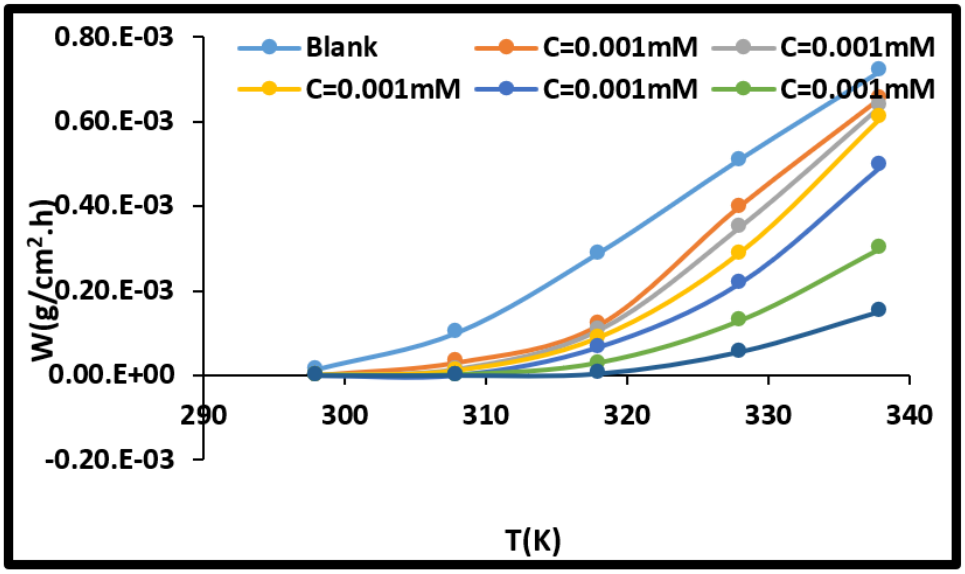

Figure 2. Curve showing the corrosion rate as a function of temperature for different concentrations of the 4Cl-BNH-NIP molecule.

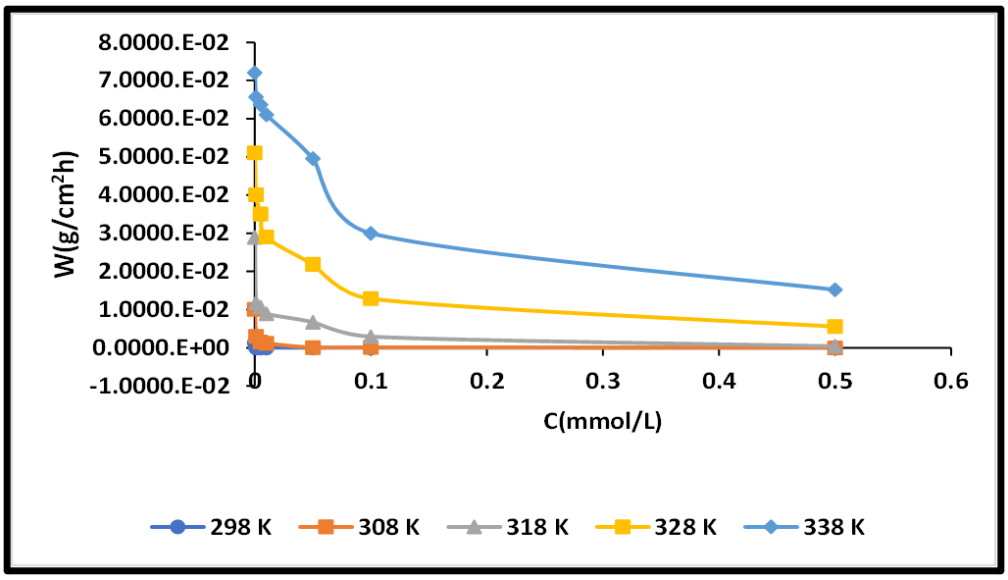

Figure 3. The curve showing the corrosion rate as a function of concentration for 4Cl-BNH-NIP at different temperatures.

By examining the two curves above, we observe that the corrosion rate, for a given inhibitor concentration, increases as the temperature rises. However, this increase in corrosion rate is relatively small for 4Cl-BNH-NIP. A protective barrier is therefore formed by adsorption of 4Cl-BNH-NIP on the aluminum surface [13].

Figures 4 and 5 show, respectively, the variation in inhibition efficiency as a function of temperature and 4Cl-BNH-NIP concentration.

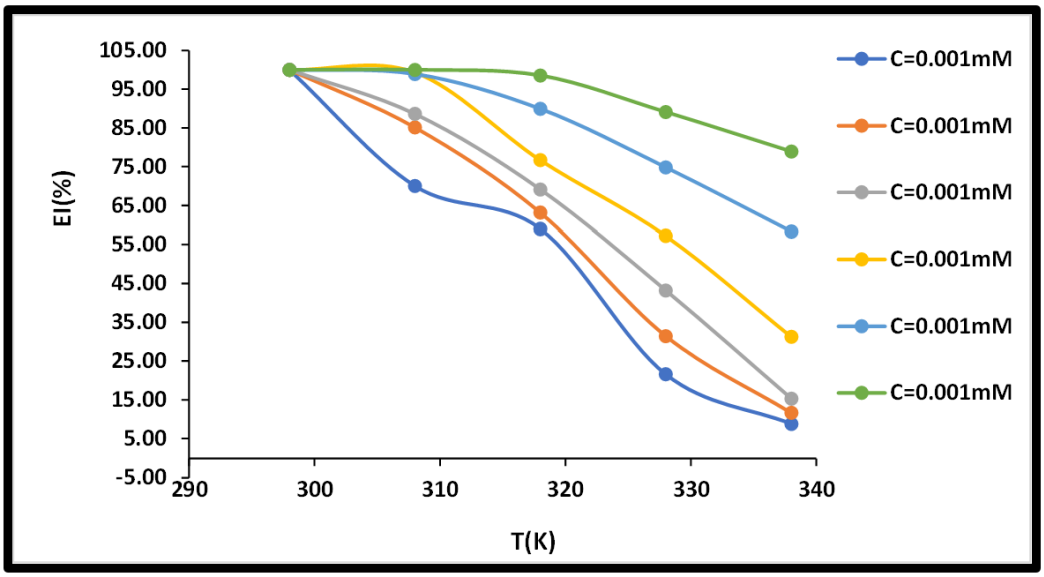

Figure 4. Inhibition efficiency as a function of temperature for different concentrations of 4Cl-BNH-NIP.

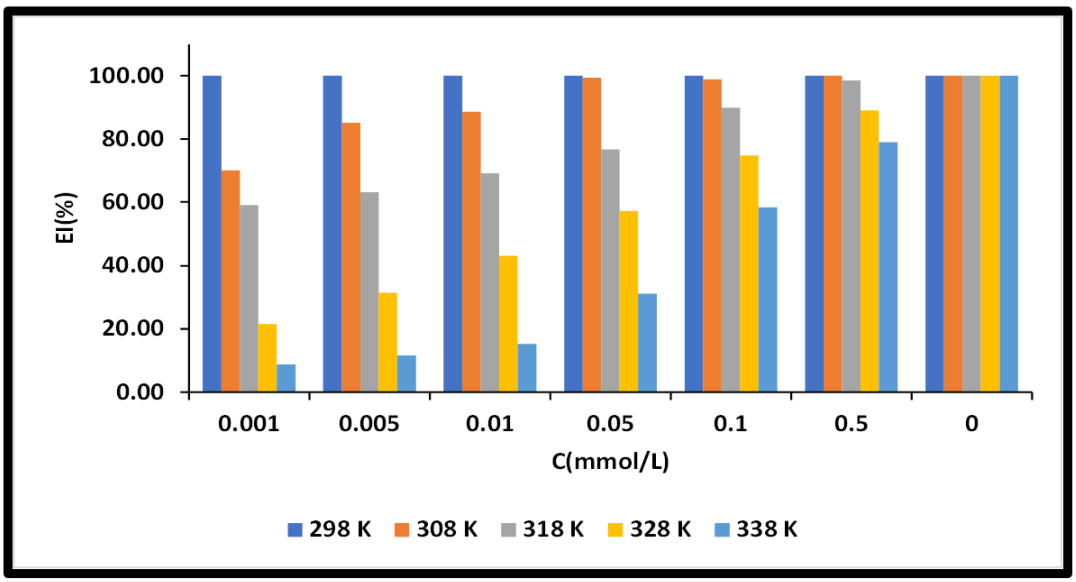

Figure 5. Band plot of the effectiveness of the 4Cl-BNH-NIP inhibitor as a function of concentration at a given temperature in an HCl medium.

Figures 4 and 5 show that the inhibitory effectiveness (EI) decreases as the temperature rises. This effectiveness also increases with increasing concentration. The increase in inhibitor concentration promotes the formation of a protective film on the substrate surface. This inhibitor density in the reaction medium ensures that the protective film reforms immediately after dissolution due to temperature elevation or resorption immediately following desorption of molecules from the metal surface [14].

3.2. Adsorption Isotherms

The selection of the most appropriate adsorption model is based on the value of the coefficient of determination R^2 obtained from the experimental plots: the higher this value, the more accurately the model describes the phenomenon under study.

$$f(\theta,x)\exp(-2a\theta) = K_{ads}C_{inh} \quad (4)$$

where $f(\theta,x)$ represents the configuration factor and depends on the physical model and the assumptions underlying the model's derivation, θ is the coverage rate of the metal surface, C_{inh} is the inhibitor concentration, a is a molecular interaction parameter, x is the number of water molecules replaced by an organic molecule, and K_{ads} is the equilibrium constant of the adsorption process. The equations for the various models are listed in Table 1 below:

Table 1. Equations for the isotherms studied.

Isotherms	Equations
Langmuir	$\frac{C_{inh}}{\theta} = \frac{1}{K_{ads}} + C_{inh}$
Temkin	$\theta = \frac{2.303}{f}[logK_{ads} + logC_{inh}]$
El-Awady	$log\left(\frac{\theta}{1-\theta}\right) = logK + y\ logC_{inh}$
Freundlich	$log(\theta) = logK_{ads} + n\ logC_{inh}$

Here,

C_{inh} is the inhibitor concentration;

K_{ads} is the equilibrium constant of the adsorption process;

f is a factor representing the energy inhomogeneity of the surface;

θ is the surface coverage;

$$K_{ads} = K'^{1/y}$$

$1/y$ is the number of active sites occupied by an inhibitor molecule.

Figures 6, 7, 8, and 9 show graphs of the isotherms studied.

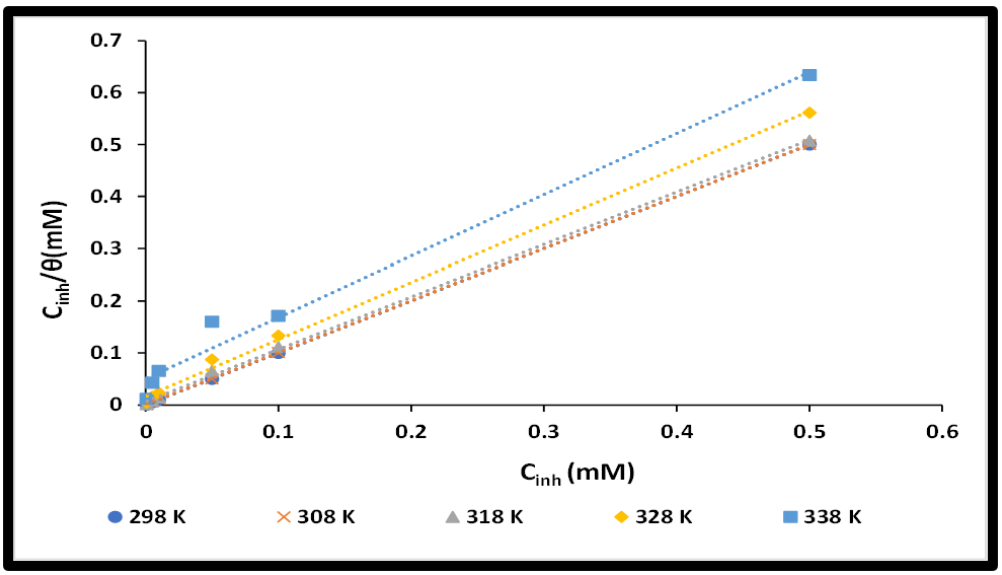

Figure 6. Langmuir isotherms for the adsorption of 4Cl-BNH-NIP on aluminum in 1 M HCl at different temperatures.

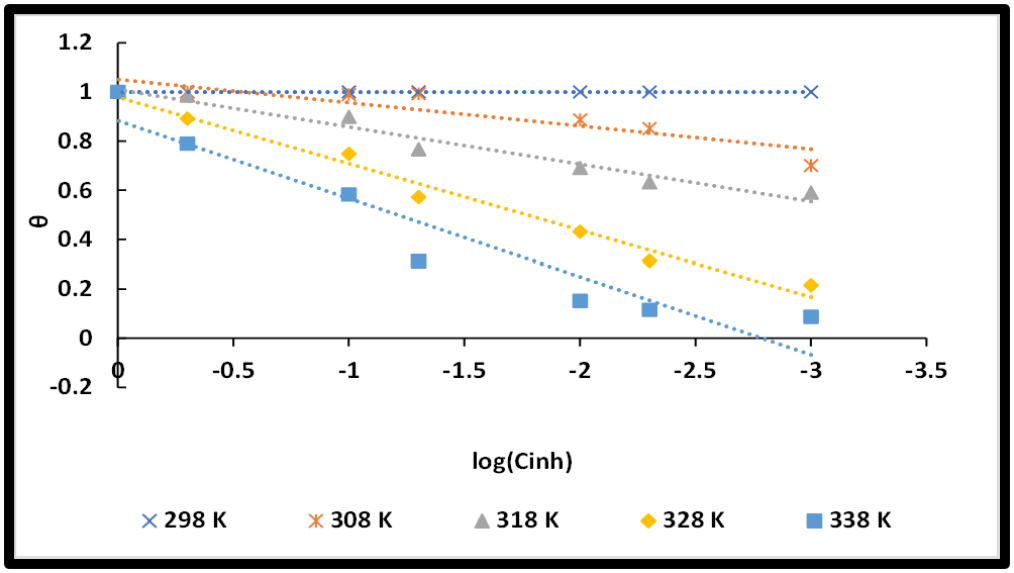

Figure 7. Temkin isotherms for the adsorption of 4Cl-BNH-NIP on aluminum in 1 M HCl at different temperatures.

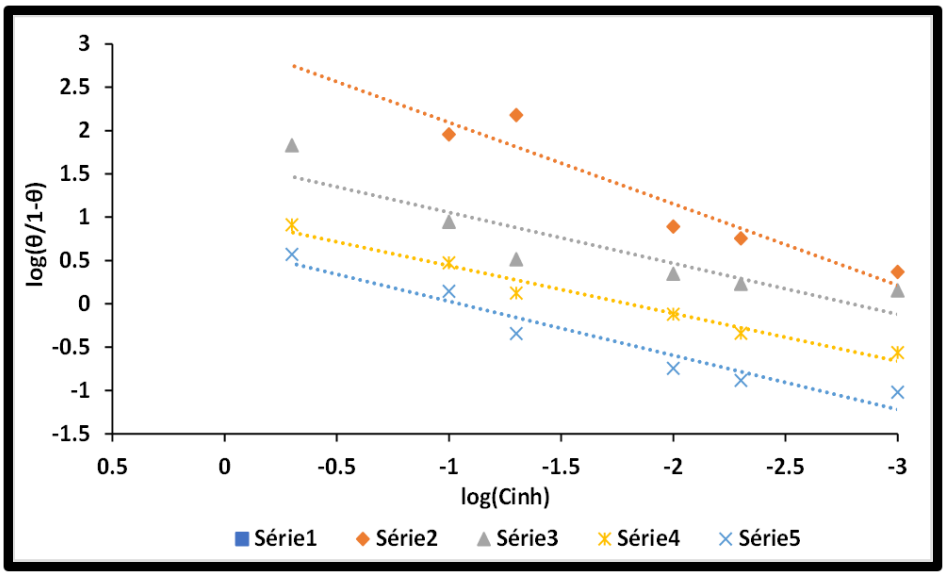

Figure 8. El-Awady isotherms for the adsorption of 4Cl-BNH-NIP on aluminum in 1 M HCl at different temperatures.

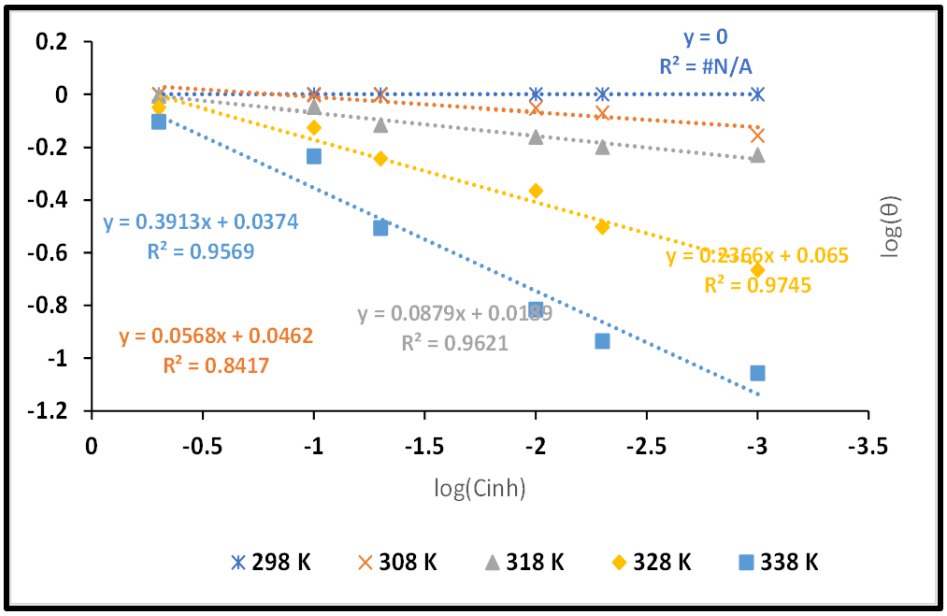

Figure 9. Dubinin-Raduskevich isotherm for the 4Cl-BNH-NIP molecule in HCl solution.

Table 2 below shows the correlation coefficients of the adsorption isotherms for the 4Cl-BNH-NIP molecule as a function of temperature in hydrochloric acid solution.

Table 2. Correlation coefficients of the adsorption isotherms for the 4Cl-BNH-NIP molecule as a function of temperature in a hydrochloric acid medium.

T(K)	Langmuir	Temkin	El Awady	Freundlich	Adejo-Ekwenchi	Dubinin-Raduskevit
298K	**1**					0,9793
308K	**1**	0,8201	0,8961	0,8417	0,8775	0,9395
318K	**0,9993**	0,9607	0,8155	0,9621	0,7719	0,8234
328K	**0,9976**	0,9824	0,9697	0,9745	0,8881	0,7534
338K	**0,9833**	0,9055	0,9331	0,9569	0,8069	0,7976

Analysis of the tables shows that the correlation coefficients (R^2) of the Langmuir isotherm are very close to 1. This indicates that this model generally provides a good description of the adsorption mechanism of inhibitors in the corrosive environments studied [14-15]. According to this model, adsorption occurs as a monolayer on the metal surface. The adsorption sites are limited in number, energetically equivalent, and each site can bind only a single inhibitor molecule. In some cases, the slopes of the lines derived from the Langmuir isotherm are greater than 1. This situation indicates that the Langmuir model is not strictly followed, consistent with the literature [15]. When these deviations occur, the actual adsorption mechanism resembles that proposed by Villamil [16]. It implies that the adsorbed molecules interact with one another, which contradicts the fundamental assumption of the Langmuir model (absence of lateral interactions). The Langmuir model remains relevant for describing overall adsorption, but certain experimental deviations reveal the existence of interactions between adsorbed molecules, suggesting a more complex mechanism than initially assumed.

This model is represented by the equation:

$$\frac{C_{inh}}{\theta} = \frac{n}{K} + nC_{inh} \tag{5}$$

$n\theta$ represents the effective coverage.

3.3. Determination of Thermodynamic Parameters Related to the Adsorption of 4Cl-BNH-NIP on Aluminum

Knowledge of the appropriate adsorption isotherm allows for the determination of the thermodynamic parameters of adsorption. The change in adsorption enthalpy ΔG^0_{ads} was calculated using the following equation:

$$\Delta G^0_{ads} = -RTln(55{,}5K_{ads}) \tag{6}$$

where R is the ideal gas constant, T is the absolute temperature, and 55.5 is the water concentration in mol/L, the obtained values of ΔG^0_{ads} are listed in Table 3 below:

Table 3. Values of thermodynamic parameters related to the adsorption of 4Cl-BNH-NIP on aluminum

T(K)	K_{ads} (M^{-1})	ΔG^0_{ads} (kJ.mol^{-1})	ΔH^0_{ads} (kJ.mol^{-1})	ΔS^0_{ads} (J.mol^{-1}.K^{-1})
298	946111.601	- 17.58	-20.415	70.4
308	846078.250	- 21.36		
318	196078.430	-20.82		
328	357466.667	-45.80		
338	124137.255	-44.23		

We observe very high values of the adsorption constant across the entire temperature range, particularly at 298 K and 308 K. These high values indicate a very large number of 4Cl-BNH-NIP molecules adsorbed onto the metal surface, especially at 298 K and 308 K [17]. Similarly, we observe negative values for the free enthalpy of adsorption across the entire temperature range studied. This would imply that the adsorption of 4Cl-BNH-NIP molecules onto the metal surface in a sulfuric acid medium occurs spontaneously [17]. The negative value of the adsorption enthalpy indicates that the process is exothermic, while the positive value of the adsorption entropy characterizes the disorder that occurs at the metal surface during the process, likely due to the desorption of water molecules from the metal surface [18]. According to the literature, a value of ΔG^0_{ads} less than -40 kJ·mol^{-1} would indicate a chemical adsorption process (chemisorption), whereas a value greater than or close to −20 kJ·mol^{-1} would rather indicate a physical adsorption process (physisorption). For values between -40 kJ·mol^{-1} and -20 kJ·mol^{-1}, both types of adsorption would occur [19]. In our present case, there is a predominance of physisorption.

The changes in adsorption enthalpy ΔH^0_{ads} and entropy ΔS^0_{ads} are calculated using the following equation:

$$\Delta G^0_{ads} = \Delta H^0_{ads} - T\Delta S^0_{ads} \quad (7)$$

where ΔH^0_{ads} and ΔS^0_{ads} are, respectively, the y-intercept and the negative slope of the line obtained from the curve showing the variation of ΔG^0_{ads} as a function of temperature (Figure 10).

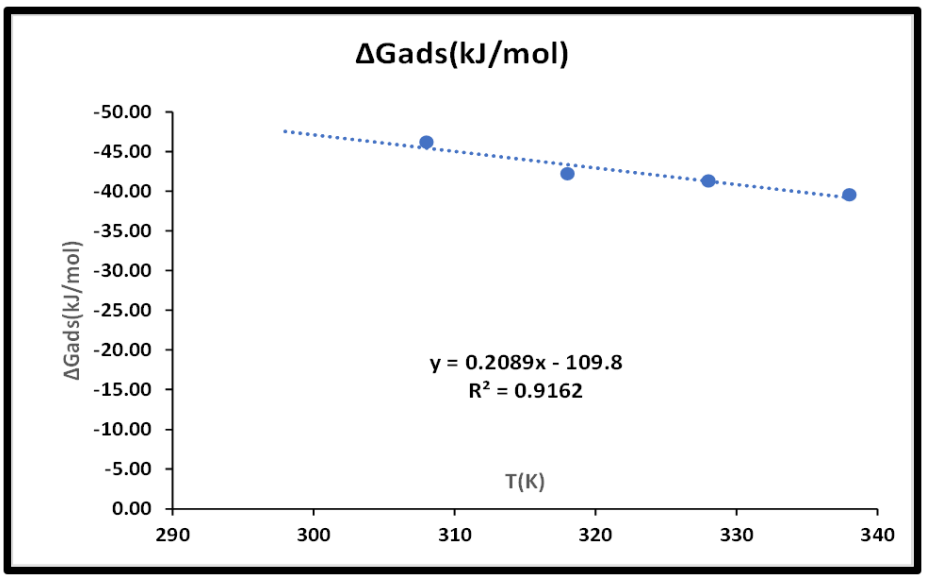

Figure 10. Variation of ΔG^0_{ads} as a function of temperature.

The negative values of the free enthalpy of adsorption demonstrate the spontaneous nature of the adsorption phenomenon. Figure 10 shows that the graph of ΔG^0_{ads} versus temperature is a straight line with a slope ($-\Delta S^0_{ads}$) and a y-intercept ΔH^0_{ads}). From the equation of this line, we find that ΔH^0_{ads}= -20.415 kJ·mol^{-1} and ΔS^0_{ads} = 70.4 J·mol^{-1} K^{-1}. The negative sign of the change in adsorption enthalpy indicates an exothermic adsorption process, while the positive sign of the change in entropy shows that disorder increases during the adsorption phase, likely due [20] to the desorption of water molecules.

Type of adsorption

To interpret the adsorption mode of our molecule, we used the Adejo-Ekwenchi and Dubinin-Radushkevich isotherms, with the respective equations:

To interpret the adsorption mechanism of our molecule, we used the Adejo-Ekwenchi and Dubinin-Radushkevich isotherms, which are described by the following equations:

$$\log[1/(1-\theta)] = logK_{AE} + b\ logC \tag{8}$$

Where KAE and b are the parameters of the isotherm, and C is the concentration of the adsorbate.

$$\text{with :} \quad \delta = RTln\left(1 + \frac{1}{MC_{inh}}\right) \tag{9}$$

$E^m_{ads} = \frac{1}{\sqrt{2a}}$ (Average adsorption energy in kJ/mol)

To confirm the type of adsorption by which the inhibitor binds to metal surfaces, we determined the parameters of the Adejo-Ekwenchi isotherm as a function of temperature in various aggressive media. Figure 11 shows the curve of log (1/1 - θ) as a function of log C. The values of all associated parameters are listed in Table 4 below:

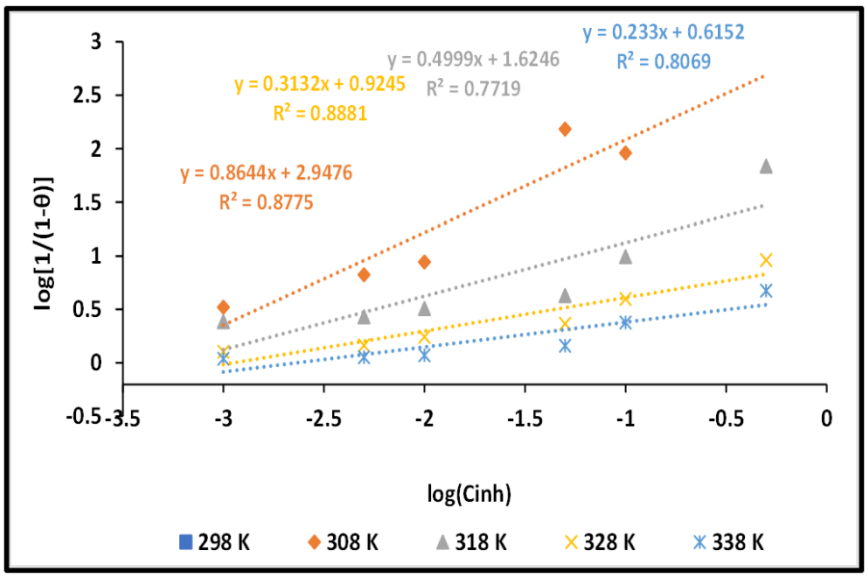

Figure 11. Adejo-Ekwenchi isotherm curves for 4Cl-BNH-NIP in HCl solution.

Table 4 below shows the parameters of the Adejo-Ekwenchi adsorption isotherm.

Table 4. Parameters of the Adejo-Ekwenchi adsorption isotherm

T(K)	K_{AE}	b
298		
308	886.3392	0.8644
318	42.1308	0.4999
328	8.4043	0.3132
338	4.1229	0.233

This table also shows that the indicator parameter b is not relatively constant. This indicates adsorption of 4Cl-BNH-NIP molecules, with physisorption predominating in a hydrochloric acid medium [21].

3.4. Activation Parameters of the Corrosion Process

The thermodynamic activation parameters (activation energy E_a, activation enthalpy change ΔH_a^* and activation entropy change ΔS_a^* for the corrosion process were determined using the Arrhenius and transition state equations [23]:

$$\mathrm{LogW} = \mathrm{logA} - \frac{\mathrm{E_a}}{2{,}3\mathrm{RT}} \tag{10}$$

$$log\left(\frac{W}{T}\right) = \left[log\left(\frac{R}{\aleph h}\right) + \frac{\Delta S_a^*}{2{,}303R}\right] - \frac{\Delta H_a^*}{2{,}303RT} \tag{11}$$

W is the corrosion rate, R is the ideal gas constant, A is the pre-exponential factor, h is Planck's constant, and $\aleph$ is Avogadro's constant; E_a activation energy, ΔH_a^*, activation enthalpy change, and ΔS_a^* activation entropy change.

Figure 12 shows the Arrhenius curves of log W versus 1/T for aluminum in a 1 M HCl solution with and without different concentrations of our inhibitor. The straight lines were obtained with correlation coefficients ($R^2 > 0.9$). The slopes ($-\frac{\mathrm{E_a}}{2{,}3\mathrm{RT}}$) of these lines are used to calculate the apparent activation energy (E_a). The values of the thermodynamic activation parameters are given in Table 5.

Table 5. Thermodynamic parameters for the dissolution of aluminum in 1 M HCl with and without different concentrations of the 4Cl-BNH-NIP inhibitor.

Concentration (mM)	$E_a(kJ.mol^{-1})$	$\Delta H_a^*(kJ.mol^{-1})$	$\Delta S_a^*(J.mol^{-1}.K^{-1})$
Blanc	81.13	78.49	-31.87
C=0.001	90.84	88.16	-5.85
C=0.005	108.22	105.54	46.02
C=0.01	113.94	111.26	62.36
C=0.05	183.88	181.20	271.59
C=0.1	159.53	156.85	193.30
C=0.5	160.93	158.21	189.49

Figure 12 below shows log (W/T) versus 1/T

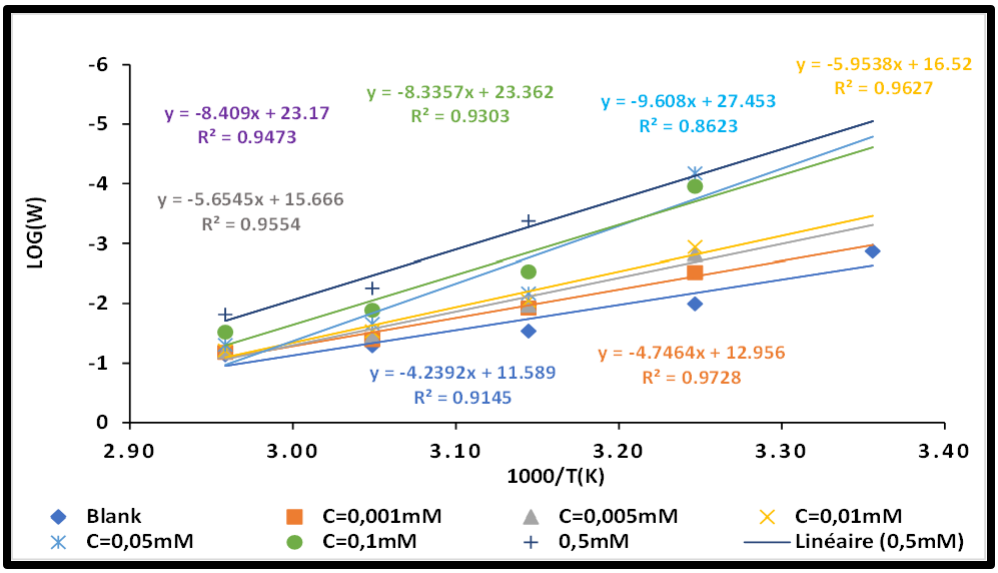

Figure 12. Variation of log W as a function of 1/T for different concentrations.

We observe, in the table, positive values and an increase in activation enthalpy across the entire range of inhibitor concentrations as the concentration increases. We also observe increasing values of activation entropy as the inhibitor concentration increases, but negative entropies at temperatures of 298 K and 3038 K. The positive values of the activation enthalpy indicate that the formation of the activated complex occurs through energy absorption. In fact, the formation of the complex reflects the dissolution of aluminum metal in the corrosive medium [22]. It is an endothermic process. The increase in activation entropy reflects disorder due to the dissolution of the formed complex or the dissolution of the metal [22].

Conclusion

In this study, the results obtained show that:

- 4Cl-BNH-NIP acts as an effective inhibitor of aluminum corrosion in a 1M hydrochloric acid medium. Its inhibitory efficiency (EI %) depends on concentration and temperature.

- 4Cl-BNH-NIP adsorbs onto aluminum according to the modified Langmuir isotherm. The calculated thermodynamic parameters related to adsorption and activation show that the predominant adsorption mode is physisorption.

References

[1] Davis, J. R. (Ed.). (1993). *Aluminum and aluminum alloys*. Materials Park, OH: ASM International, pp. 1–784.

[2] Polmear, I. J. (2006). *Light alloys: metallurgy of the light metals* (4th ed.). Oxford, UK: Butterworth-Heinemann, pp. 1–421. https://doi.org/10.1016/B978-075066371-7/50005-0

[3] Fontana, M. G. (2005). *Corrosion engineering* (3rd ed.). New York, NY: McGraw-Hill, pp. 1–556.

[4] Revie, R. W., & Uhlig, H. H. (2008). *Corrosion and corrosion control: an introduction to corrosion science and engineering* (4th ed.). Hoboken, NJ: John Wiley & Sons, pp. 1–512. https://doi.org/10.1002/9780470277270

[5] Landolt, D. (2007). *Corrosion and surface chemistry of metals*. Lausanne, Switzerland: EPFL Press, pp. 1–615. https://doi.org/10.1201/9781439807880

[6] CETIM. (2021). *Rapport sur les coûts de la corrosion*. Senlis, France: Centre Technique des Industries Mécaniques, pp. 1–98.

[7] Obot, I. B., Macdonald, D. D., & Gasem, Z. M. (2015). Density functional theory (DFT) as a powerful tool for designing new organic corrosion inhibitors. *Corrosion Science*, *99*, 1–30. https://doi.org/10.1016/j.corsci.2015.01.037

[8] Bentiss, F., Traisnel, M., & Lagrenée, M. (2000). The substituted 1,3,4-oxadiazoles: A new class of corrosion inhibitors of mild steel in acidic media. *Corrosion Science*, *42*(1), 127–146. https://doi.org/10.1016/S0010-938X(99)00049-9

[9] ASTM International. (2004). *ASTM G31-72(2004): Standard practice for laboratory immersion corrosion testing of metals*. West Conshohocken, PA: ASTM International, pp. 1–8.

[10] Khadom, A. A., Yaro, A. S., & Kadhum, A. A. H. (2010). Corrosion inhibition by naphthylamine and phenylenediamine for the corrosion of copper-nickel alloy in hydrochloric acid. *Journal of the Taiwan Institute of Chemical Engineers*, *41*(1), 122–125. https://doi.org/10.1016/j.jtice.2009.08.001

[11] Musa, A. Y., Khadom, A. A., Kadhum, A. A. H., Mohamad, A. B., & Takriff, M. S. (2010). Kinetic behavior of mild steel corrosion inhibition by 4-amino-5-phenyl-4H-1,2,4-triazole-3-thiol. *Journal of the Taiwan Institute of Chemical Engineers*, *41*(1), 126–128. https://doi.org/10.1016/j.jtice.2009.08.002

[12] Rahim, A. A., & Kassim, J. (2008). Recent development of vegetal tannins in corrosion protection of iron and steel. *Recent Patents on Materials Science*, *1*(3), 223–231. https://doi.org/10.2174/1874464810801030223

[13] Touré, R. H., Koffi, A. A., Tigori, M. A., & Niamien, P. M. (2024). Investigation on the properties of methyl 4-(((1H-benzimidazol-2-yl)methyl)thio)methyl benzoate on aluminum corrosion in acidic environment. *American Journal of Applied Chemistry*, *12*(6), 135–148. https://doi.org/10.11648/j.ajac.20241206.12

[14] Yeo, M., Tigori, M. A., Kouyaté, A., Niamien, P. M., & Trokourey, A. (2020). Inhibition of aluminium corrosion in 1 M HCl by pyridoxine hydrochloride: Thermodynamic and quantum chemical studies. *International Research Journal of Pure and Applied Chemistry*, *21*(21), 20–38. https://doi.org/10.9734/irjpac/2020/v21i2130286

[15] N'Guessan, Y. S., Gbe, G. D., Lemeyonouin, A. G., Niamien, P. M., & Trokourey, A. (2018). Aluminum corrosion inhibition by 7-(ethylthiobenzimidazolyl) theophylline in 1 M hydrochloric acid: Experimental and DFT studies. *International Journal of Applied Pharmaceutical Sciences and Research*, *3*(1), 41–53. https://doi.org/10.21477/ijapsr.3.4.1

[16] Villamil, R. F. V., Corio, P., Rubin, J. C., & Agostinho, S. M. L. (1999). Effect of sodium dodecyl sulfate on copper corrosion in sulfuric acid media in the absence and presence of benzotriazole. *Journal of Electroanalytical Chemistry*, *472*(1–2), 112–116. https://doi.org/10.1016/S0022-0728(99)00267-3

[17] Fiala, A., & Mechehoud, Y. (2012). Étude de l'effet inhibiteur du 2-(1,3-dithiétan-2-ylidène)-3-oxobutanoate de méthyle et du 2-(1,3-dithiolane-2-ylidène)-3-oxobutanoate de méthyle sur la corrosion du cuivre en milieu nitrique 3 mol·L^{-1}. *Sciences & Technologie, Section A*, *35*, 23–30.

[18] Bockris, J. O'M., & Reddy, A. K. N. (1977). *Modern electrochemistry*. New York, NY: Plenum Press, pp. 1–834.

[19] Gece, G. (2008). The use of quantum chemical methods in corrosion inhibitor studies. *Corrosion Science*, *50*(11), 2981–2992. https://doi.org/10.1016/j.corsci.2008.08.043

[20] Banerjee, G., & Malhotra, S. N. (1992). Contribution to the adsorption of corrosion inhibitors on metal surfaces. *Corrosion Science*, *32*(10), 1051–1060. https://doi.org/10.5006/1.3315912

[21] Touré, H. R., Bamba, A., Ehouman, A. D., & Niamien, P. M. (2024). Study of the inhibitory properties of 2-((benzylthio)methyl)-1H-benzo[d]imidazole with respect to the corrosion of aluminum in a nitric acid medium. *Earthline Journal of Chemical Sciences*, *11*(3), 471–487. https://doi.org/10.34198/ejcs.11324.471487

[22] Aphouet, A. K., N'Guadi, B. A., Mougo, A. T., Teminfolo, Y. S., Trokourey, A., & Niamien, P. M. (2023). Study of expired Fuclo 500 drug as an environmentally sustainable corrosion inhibitor. *European Journal of Chemistry*, *14*(3), 353–361. https://doi.org/10.5155/eurjchem.14.3.353-361.2443

This is an open access article distributed under the terms of the Creative Commons Attribution License (http://creativecommons.org/licenses/by/4.0/), which permits unrestricted, use, distribution and reproduction in any medium, or format for any purpose, even commercially provided the work is properly cited.